The Astrophysical Journal, 698:L51–L55, 2009 June 10 doi:10.1088/0004-637X/698/1/L51

CORONAL MASS EJECTIONS AND GLOBAL CORONAL MAGNETIC FIELD RECONFIGURATION

Ying Liu[1], Janet G. Luhmann[1], Robert P. Lin[1], Stuart D. Bale[1], Angelos Vourlidas[2], and Gordon J. D. Petrie[3]
[1] Space Sciences Laboratory, University of California, Berkeley, CA 94720, USA; liuxying@ssl.berkeley.edu.
[2] Space Science Division, Naval Research Laboratory, Washington, DC 20375, USA
[3] National Solar Observatory, Tucson, AZ 85719, USA
Received 2009 April 1; accepted 2009 May 7; published 2009 May 21

ABSTRACT

We investigate the role of coronal mass ejections (CMEs) in the global coronal magnetic field reconfiguration, a debate that has lasted for about two decades. Key evidence of the coronal field restructuring during the 2007 December 31 CME is provided by combining imaging observations from widely separated spacecraft with the potential-field source-surface (PFSS) model, thanks to the extraordinarily quiet Sun at the present solar minimum. The helmet streamer, previously disrupted by the CME, re-forms but is displaced southward permanently; the preexisting heliospheric plasma sheet (HPS) is also disrupted as evidenced by the concave-outward shape of the CME. The south polar coronal hole shrinks considerably. Plasma blobs moving outward along the newly formed HPS suggest the occurrence of magnetic reconnection between the fields blown open by the CME and the ambient adjacent open fields. A streamer-like structure is also observed in the wake of the CME and interpreted as a plasma sheet where the thin post-CME current sheet is embedded. These results are important for understanding the coronal field evolution over a solar cycle as well as the complete picture of CME initiation and propagation.

Key words: Sun: corona – Sun: coronal mass ejections (CMEs) – Sun: magnetic fields

Online-only material: mpeg animations

1. INTRODUCTION

Coronal mass ejections (CMEs) are large-scale expulsions of plasma and magnetic field from the solar corona. One of the most intriguing questions concerning CMEs is their relationship to the evolution of the global coronal magnetic field configuration. While people tend to believe that CMEs are a consequence of the coronal field rearrangement due to a loss of stability of the field (e.g., Forbes 2000, and references therein), debate exists as to whether CMEs respond passively or contribute dynamically to the coronal field restructuring.

Early CME observations show that many CMEs originate from the disruption of helmet streamers (e.g., Illing & Hundhausen 1986; Hiei et al. 1993; Hundhausen 1993). A helmet streamer is a cusp-like structure commonly observed in coronagraph images that separates coronal holes of opposite magnetic polarity. These observations lead to the "traditional" picture of CME eruption as suggested by Low (1996): closed fields underneath a streamer are stressed by some mechanisms to the point of instability. This picture, which forms the basis of most global MHD modeling of CMEs (e.g., Gibson & Low 1998; Wu et al. 1999; Manchester et al. 2004), is theoretically appealing as it relates a diversity of phenomena including streamers, prominences, flares, and CMEs. While Low (1996, 1997, 2001) emphasizes that the polarity reversal of the Sun over an 11-year cycle is driven by the interior dynamo, he considers CMEs as a basic mechanism of coronal magnetic field reconfiguration: CMEs remove the old magnetic flux and helicity from the corona to make room for the flux of the new cycle; each CME contributes a permanent change to the coronal field configuration so as to completely reverse the field polarity over a solar cycle. This hypothesis is contrary to the suggestion of Sime (1989) that the global coronal field organization does not respond in a lasting way to CMEs based on the argument that the mass and energy of a CME are much smaller than those of the corona. As Low (1996, 1997, 2001) envisions, CMEs are not a significant mass-loss process but far more important as a means to remove magnetic flux and helicity that would otherwise build up in the corona.

These two opposing hypotheses remain largely untested, although studies favoring one or the other have been presented. Gopalswamy et al. (2003) observe a close correlation between the cessation of high-latitude CMEs and the polar field reversal; polar crown filaments, representative of closed field structures, need to be removed for the polarity reversal to be completed, which is consistent with the hypothesis of Low (1996, 1997, 2001). Examination of images from the Large Angle Spectroscopic Coronagraph (LASCO) aboard the *Solar and Heliospheric Observatory* (*SOHO*) shows that 63% of the CMEs from 1996 January to 1998 June are associated with streamers whereas most of them have no apparent effect on the streamer (Subramanian et al. 1999). Zhao & Hoeksema (1996) find that the heliospheric current sheet (HCS) obtained with the potential-field source-surface (PFSS) model is essentially unchanged before and after CMEs in the declining phase of solar cycle 21; the streamer belt re-forms in a timescale of about 2 days. A more recent study, however, argues that the global coronal field topology is prone to major reconfigurations; even a single bipolar active region artificially introduced into the background field can significantly change the global coronal field geometry (Luhmann et al. 2003). The insensitivity of the coronal field configuration to CMEs would be difficult to reconcile in this context.

Now that we have three spacecraft looking at the Sun including *SOHO* and *STEREO*, the effects of CMEs on the preexisting streamers may be observed more fully. In particular, the *STEREO* twin spacecraft, one preceding the Earth (*STEREO A*) and the other trailing behind (*STEREO B*), provide widely separated views of the Sun off the Sun–Earth line. The focus of this Letter is to combine these imaging observations with PFSS modeling to present evidence for global coronal field reconfiguration during some CMEs. The results obtained here are also

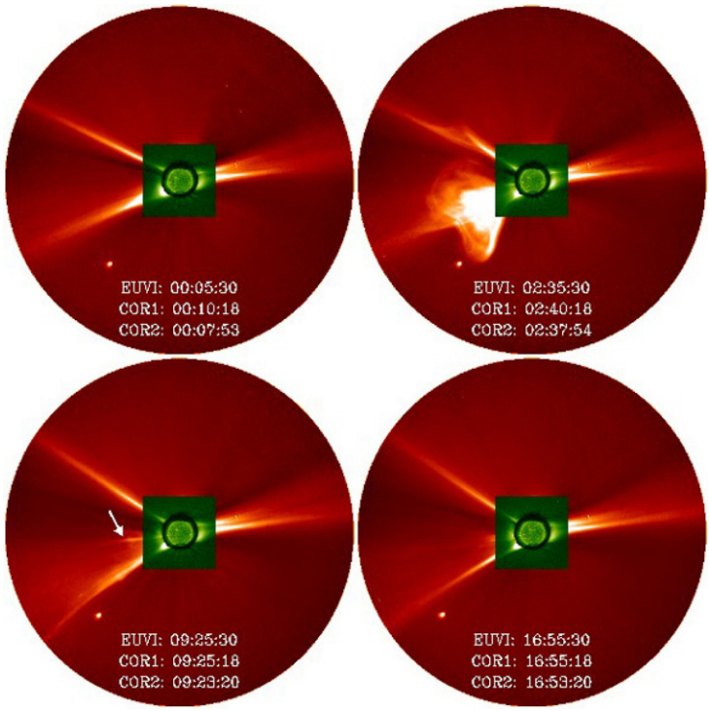

Figure 1. Composite images of EUVI at 195 Å, COR1 and COR2 aboard *STEREO A* showing the coronal configuration before, during, and after the CME on 2007 December 31. The arrow indicates the post-CME plasma sheet. Note the plasma blobs moving outward along the newly formed HPS and the post-CME plasma sheet. The solar ecliptic north is up.

(An mpeg animation of this figure is available in the online journal.)

crucial for understanding the complete picture of CME initiation and propagation.

2. OBSERVATIONS AND MODELING

Coronal field reconfigurations during CMEs are best studied at solar minimum when the corona has a relatively simple configuration and effects of individual CMEs can be isolated. During the current solar minimum, the Sun has been extraordinarily quiet, for example, lowest radio flux since 1947, lowest solar wind ram pressure since the beginning of the space era (e.g., McComas et al. 2008), and effectively no sunspots. The CME occurrence rate is typically below 0.5 per day at the present solar minimum (see http://cor1.gsfc.nasa.gov/catalog/). This provides an unprecedented opportunity to characterize the global coronal field reconfiguration. The PFSS model (e.g., Schatten et al. 1969; Altschuler & Newkirk 1969; Altschuler et al. 1977; Wang & Sheeley 1992) is used to construct the coronal fields based on standard synoptic magnetograms observed by the Global Oscillation Network Group (GONG). Note that the synoptic field map cannot capture the dynamical transition between two adjacent states. The extremely slow evolution of the solar field at this particular solar minimum makes it possible to investigate the coronal field reconfiguration during CMEs under the assumption that such reconfigurations can persist for a long enough time to be recognized in the PFSS modeling. Additional confidence is provided by aligning the PFSS modeled structure with observed images (see below).

The 2007 December 31 CME is the most conspicuous event during Carrington rotations (CRs) 2063–2065. Figure 1 shows composite images from the Extreme Ultraviolet Imagers (EUVI) and the coronagraphs (COR1 and COR2) of the Sun Earth Connection Coronal and Heliospheric Investigation (SECCHI) aboard *STEREO A*. Two ray structures are apparent at the east limb before the CME, which correspond to a pseudostreamer (upper) and the streamer belt (lower) seen by *STEREO A*. A pseudostreamer also has a cusp-like field structure but is local, rather than global, and separates open field lines of the same polarity (Wang et al. 2007). The field configuration around the pseudostreamer is shown in the Appendix. The CME emerges as a semicircular structure from the coronal base of the helmet streamer (Liu et al. 2009). The initiation of the CME is consistent with the traditional scenario suggested by Low (1996). The bright stalk at the tip of the streamer belt is likely the heliospheric plasma sheet (HPS), a layer around the HCS with increased mass density (Winterhalter et al. 1994). One of the most striking features in Figure 1 is the denting of the CME into a concave-outward shape, indicative of a strong interaction between the CME and the preexisting HPS. This is an important point missed by previous CME observations: CMEs erupting beneath the streamer belt disrupt not only the streamer but also the preexisting HCS (and hence the HPS). Therefore, the global field configuration of the heliosphere will also be altered. The denting begins at a few solar radii, where we expect that it is not due to the solar wind speed gradient (as in the solar wind further out) but rather the HPS that acts like an obstacle (also see Liu et al. 2006, 2008). As a result, the CME speed shows a clear latitudinal variation. It is about 790 km s^{-1} and 880 km s^{-1}, respectively, along directions 20° north and south of the streamer whereas only about 690 km s^{-1} along the streamer. The pseudostreamer is deflected by the CME-driven shock that forms in the low corona (Liu et al. 2009).

Of particular interest is that the streamer as well as the HPS re-forms at the south side of the CME (see the accompanying animation online), not right behind as predicted by axisymmetric MHD simulations (e.g., Wu et al. 1999; Manchester et al. 2004).

In axisymmetric simulations, magnetic reconnection occurs only between the fields blown open by the CME, so the corona relaxes exactly to the same state as before the CME; in this case, CMEs come and go without any effect on the global coronal field configuration. Figure 1 reveals a novel scenario about this particular coronal restructuring: magnetic reconnection seems to occur between the newly opened fields and the fields from the south polar coronal hole, which may be facilitated by the vast lateral expansion of the CME. Outward plasma flows along the newly formed HPS indicate the occurrence of magnetic reconnection. Owing to this reconnection the streamer belt must migrate southward and the south coronal hole should shrink. The southward migration of the streamer (as well as the HPS) is apparent in Figure 1. The streamer also becomes much thinner than before. This reconfiguration scenario may help to understand the unusually high tilt angle of the streamer belt at this solar minimum. Note that the coronal configuration does not change until the CME has occurred.

A closer look at Figure 1 reveals another ray-like stalk in the wake of the CME; plasma blobs moving outward, probably reconnection outflows, are also observed along the stalk (see the online animation). EUVI images show successively growing flare loops underneath the stalk (see Figure 3 and the corresponding animation); above the flare loop top, a hard X-ray emission source is observed by *RHESSI* (S. Krucker 2009, private communication). This may be the streamer-like structure that has been interpreted as the post-CME "current sheet" (e.g., Ko et al. 2003; Lin et al. 2007). In situ measurements show that the HCS is a very narrow layer with a typical width of about 200 proton gyroradii ($<10^4$ km), whereas the HPS (where the HCS is embedded) is about 3×10^5 km (Winterhalter et al. 1994). The typical thickness of a post-CME stalk is about 10^5 km (Lin et al. 2007), comparable to the HPS width but much larger than the HCS as measured in situ. The analogy between the HPS and the post-CME stalk that simultaneously form after the CME indicates that the streamer-like structure is probably a plasma sheet with enhanced density within which the significantly thinner post-CME current sheet is embedded; specifically, the current sheet itself is not thick enough to be observable (as a result of the high electrical conductivity and nearly force-free environment in the corona). An unusually large electric resistivity is invoked to explain the observed width of the post-CME stalk (e.g., Lin et al. 2007). The reinterpretation of the streamer-like structure behind the CME as a plasma sheet naturally explains the observed width without the need of an unrealistic electric resistivity. Note that the post-CME plasma sheet does not overlap with the newly formed HPS as in axisymmetric simulations.

The coronal field configuration resulting from the PFSS extrapolation is displayed in Figure 2 as a synoptic map. The CME originates from NOAA AR 10978 with a Carrington longitude 225° and latitude −9° beneath the streamer belt, as shown by the map of CR 2064. The change in the coronal field configuration is dramatic. The source surface neutral line (the coronal base of the HCS) during CR 2064 becomes more warped than at CR 2063; the part of the neutral line between longitudes 250° and 360° moves southward by an angle at least 10° on average. The PFSS modeled streamer belt at these longitudes also narrows down significantly. The south polar coronal hole, as indicated by the footpoints of the open fields, is considerably reduced. The global field configuration does not recover to its pre-CME state even during CR 2065, so those changes seem permanent. Some of the open flux from the south coronal hole must have closed down. The white-light structure is believed to

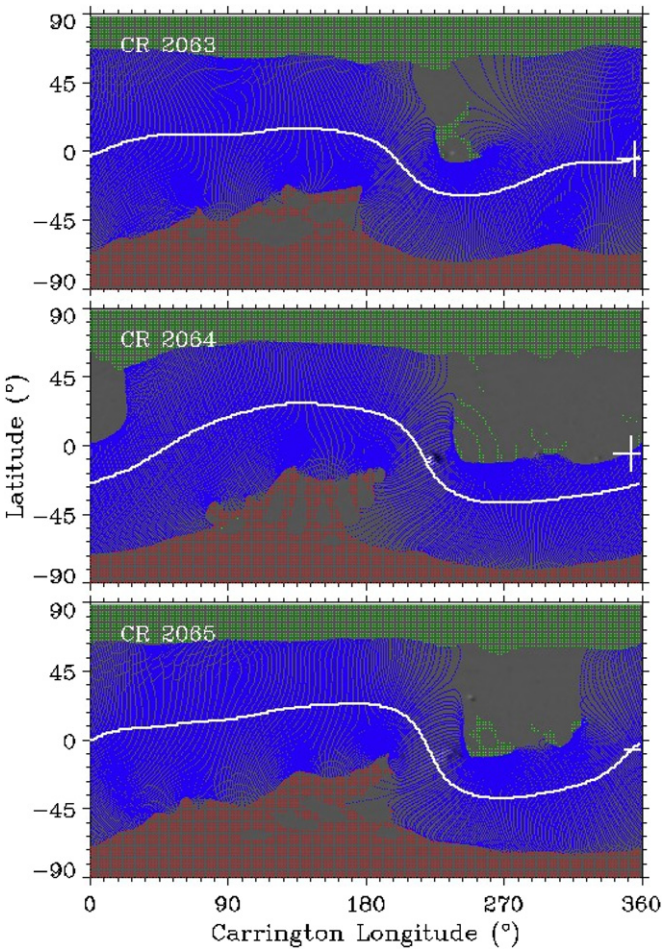

Figure 2. PFSS modeled field lines of the streamer belt (blue), footpoints of negative (green) and positive (red) open fields, and the source surface neutral line (white) projected onto the synoptic map of the photospheric field for CRs 2063–2065. The cross indicates the location of *STEREO A* in Carrington coordinates at times shown in Figure 3.

(An mpeg animation of this figure is available in the online journal.)

trace the global field configuration of the corona. The brightness at a certain point is proportional to the integral of the electron density along the line of sight, which is dominated by the electrons near the limb of the Sun (Billings 1966; Hundhausen 1993). *STEREO A* is located at a Carrington longitude of about 360° on 2007 December 31 and 2008 January 27. At the east limb, the most visible structure to *STEREO A* would be the part of the streamer belt around 270° in longitude, i.e., 90° east of the spacecraft. The changes revealed by the PFSS modeling (specifically around 270°) agree well with those as seen in Figure 1 by *STEREO A*. Therefore, these changes must have been associated with the CME.

Further confidence for the coronal field changes associated with the CME is provided by aligning the PFSS modeled structures with observed images, as illustrated in Figure 3. The PFSS modeled streamer belt lines up very well with the observed streamer; footpoints of the open field lines also agree with the polar coronal holes discernible in EUVI images. It should be stressed that the PFSS modeling for CRs 2063 and 2064, even though based on synoptic maps of the photospheric field, reproduces the observed features right before and right after the CME; this remarkable match with a one-to-one correspondence confirms the association of the coronal field reconfiguration

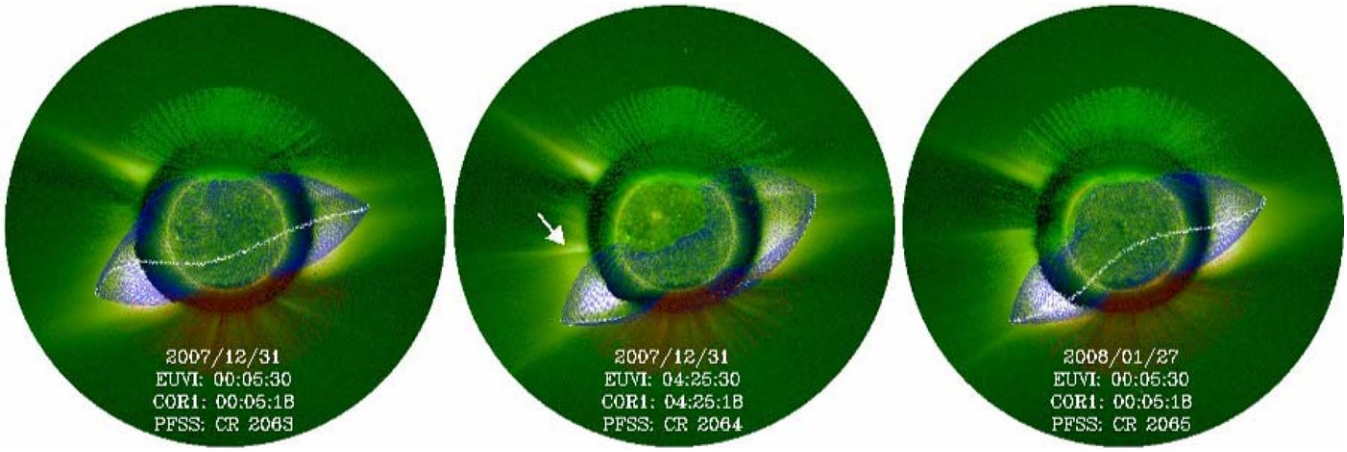

Figure 3. Composite images of EUVI at 195 Å and COR1 aboard *STEREO A* showing the coronal configuration before and after the CME on 2007 December 31 and 27 days later. The PFSS model fields and source surface neutral line for CRs 2063–2065 are projected onto the images with the same color coding as in Figure 2. The arrow indicates the post-CME plasma sheet. Note that the ray structure between the pseudostreamer and streamer on 2008 January 27 (right panel) is not the post-CME plasma sheet, which originates from a lower latitude and disappears later on 2007 December 31. The solar ecliptic north is up.

(An mpeg animation of this figure is available in the online journal.)

with the CME. The coronal reconfiguration clearly survives after the CME is over. In particular, the streamer belt that has migrated southward persists for a time even longer than a complete solar rotation, as shown by the agreement between the modeled structures for CR 2065 and the observed ones 27 days later (see the right panel). The observations on 2008 January 27 indicate that the pseudostreamer has moved back to its original position. The post-CME plasma sheet with growing flare loops under it is also visible in Figure 3 but fades away later on 2007 December 31 (see the online animation).

Observations from *STEREO B* and *SOHO* are also examined. *STEREO A* and *B* are separated by about 44° in longitude on 2007 December 31 with *SOHO* in between. A generally similar scenario (such as the concave-outward shape of the CME, the southward migration of the streamer, the deflection of the pseudostreamer and the post-CME plasma sheet) is observed by *SOHO* but less clear than *STEREO A* images. *STEREO B* observes a diffusive fan-like structure at the east limb of the Sun, which is then split by the CME; the concave-outward structure as well as the post-CME plasma sheet is detected whereas the preexisting HPS is missed. These observations are consistent with the coronal field restructuring shown in Figure 2 as would be seen by *STEREO B* and *SOHO*. The consistency between the observations from three widely separated spacecraft and the PFSS modeling pins down the CME as the only event associated with the coronal field reconfiguration.

The PFSS model uses the observed photospheric fields as boundary conditions, so any change in the photospheric fields would lead to an immediate change in the PFSS modeled coronal fields. The actual changes in the global coronal field configuration, however, could be significantly delayed. It has been suggested that new magnetic fields reaching the photosphere require about one solar rotation to make their effects known to the interplanetary medium (Schatten et al. 1969). The PFSS modeled coronal fields show the reconfiguration during CR 2064 whereas the associated CME occurs at the beginning of CR 2065 (2007 December 29–2008 January 25). This time delay indicates that, before the CME erupts, the coronal fields are simply stressed by the photospheric field changes without exhibiting an obvious global reconfiguration.

A preliminary look at LASCO CMEs in the declining phase of the last solar cycle (before the launch of *STEREO*) shows another event, which occurs on 2005 September 5 and appears to be associated with a similar coronal field rearrangement. The CME is also concave outward due to its interaction with the preexisting streamer and HPS. The streamer re-forms at the south side of the CME with plasma flows along the new HPS, indicative of magnetic reconnection between the fields opened by the CME and the ambient open fields. This closing of the fields inferred from the above observations may hold important clues for understanding the role of CMEs in the field polarity reversal in the corona.

3. CONCLUSION

We combine imaging observations with PFSS modeling to investigate the global coronal field reconfiguration associated with the 2007 December 31 CME, taking advantage of the current unusually quiet solar minimum. Two types of coronal field changes can be identified. Short-lived changes arise from a mechanical process, by which coronal structures (such as the pseudostreamer) are pushed aside and then bounce back when the CME is gone. Permanent changes result from magnetic reconnection, by which the ambient flux and the newly opened fields cancel out. This reconnection scenario is justified by the formation of double plasma sheets, i.e., the post-CME plasma sheet and the new HPS. This is a restructuring process of the corona where the streamer belt can migrate during CMEs, an effect not previously considered in CME models. These results are more or less consistent with the hypothesis of Low (1996, 1997, 2001) that CMEs may represent the basic mechanism of coronal field reconfiguration. Whether CMEs could regulate the coronal field reconfiguration systematically, however, needs further investigations.

Also note that some CMEs may simply release the accumulated local energy or stress without permanent effects on the large-scale coronal field reconfiguration. Other CMEs, such as those we look at, migrate the open/closed fields around. These are important differences, as only the latter would reflect the cycle evolution of the global field configuration in the corona. While there may be a quasi-steady evolution of the coronal open and closed fields as the photospheric fields evolve with time (e.g., due to differential rotation of the solar plasma and supergranular diffusion of bipolar magnetic regions; see Wang & Sheeley 2003, and references therein), CMEs like the latter

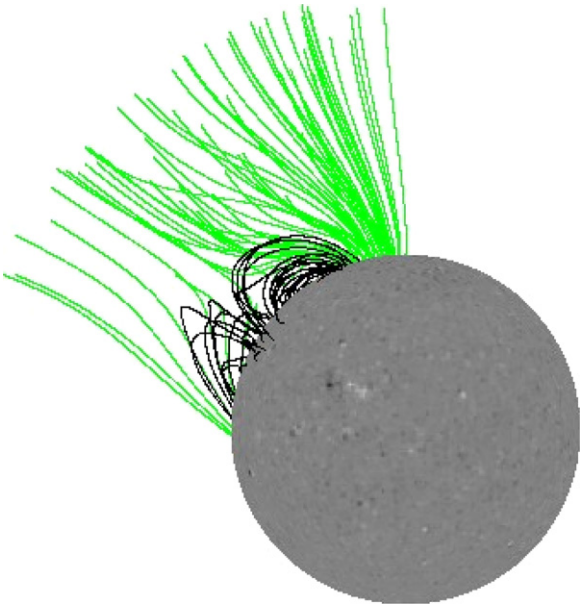

Figure 4. Field topology around the pseudostreamer on top of the photospheric field map for CR 2063 as viewed from *STEREO A* on 2007 December 31. Closed field lines are drawn in black, and open field lines directed inward are coded green.

could make fairly big changes rather quickly. Therefore, the evolution of the coronal field configuration may be a combination of slow changes punctuated by large steps from these special kinds of CMEs.

The research was supported by the *STEREO* project under grant NAS5-03131. We acknowledge the use of GONG data. Y. Liu thanks H. S. Hudson for helpful discussion. This work was also supported in part by grant NNSFC 40621003.

APPENDIX

FIELD CONFIGURATION OF THE PSEUDOSTREAMER

An equatorial coronal hole is present around the Carrington longitude 235° in the map of CR 2063 (see Figure 2). The fields between the north polar coronal hole and the equatorial one likely give rise to the pseudostreamer seen in Figure 1. The corresponding field configuration in this region is shown in Figure 4 as would be observed by *STEREO A*. Two adjacent loop arcades are evident underneath the open field lines from the coronal holes of the same polarity; the open field lines converge above the arcades to make a cusp structure. This is a typical signature of pseudostreamers (Wang et al. 2007). The axis of the double arcade seems perpendicular to the limb of the Sun, consistent with the narrow bright stalk observed by *STEREO A*. The pseudostreamer extends out to more than 30 solar radii (see Liu et al. 2009), a surprisingly large extension compared with the typical length found by Wang et al. (2007). One of the most interesting questions about a pseudostreamer is how its field geometry avails to make a plasma sheet, which can only be answered by in situ measurements from the Solar Probe Plus that will go to the Sun as close as 10 solar radii.

REFERENCES

Altschuler, M. D., Levine, R. H., Stix, M., & Harvey, J. 1977, Sol. Phys., 51, 345
Altschuler, M. D., & Newkirk, G. 1969, Sol. Phys., 9, 131
Billings, D. E. 1966, in A Guide to the Solar Corona (New York: Academic)
Forbes, T. G. 2000, J. Geophys. Res., 105, 23153
Gibson, S. E., & Low, B. C. 1998, ApJ, 493, 460
Gopalswamy, N., Lara, A., Yashiro, S., & Howard, R. A. 2003, ApJ, 598, L63
Hiei, E., Hundhausen, A. J., & Sime, D. G. 1993, Geophys. Res. Lett., 20, 2785
Hundhausen, A. J. 1993, J. Geophys. Res., 98, 13177
Illing, R. M. E., & Hundhausen, A. J. 1986, J. Geophys. Res., 91, 10951
Ko, Y.-K., et al. 2003, ApJ, 594, 1068
Lin, J., Li, J., Forbes, T. G., Ko, Y.-K., Raymond, J. C., & Vourlidas, A. 2007, ApJ, 658, L123
Liu, Y., Luhmann, J. G., Bale, S. D., & Lin, R. P. 2009, ApJ, 691, L151
Liu, Y., Manchester, W. B., Richardson, J. D., Luhmann, J. G., Lin, R. P., & Bale, S. D. 2008, J. Geophys. Res., 113, A00B03
Liu, Y., Richardson, J. D., Belcher, J. W., Wang, C., Hu, Q., & Kasper, J. C. 2006, J. Geophys. Res., 111, A12S03
Low, B. C. 1996, Sol. Phys., 167, 217
Low, B. C. 1997, Geophys. Monogr., 99, 39
Low, B. C. 2001, J. Geophys. Res., 106, 25141
Luhmann, J. G., Li, Y., Zhao, X., & Yashiro, S. 2003, Sol. Phys., 213, 367
Manchester, W. B., IV, et al. 2004, J. Geophys. Res., 109, A01102
McComas, D. J., et al. 2008, Geophys. Res. Lett., 35, L18103
Schatten, K. H., Wilcox, J. M., & Ness, N. F. 1969, Sol. Phys., 6, 442
Sime, D. G. 1989, J. Geophys. Res., 94, 151
Subramanian, P., Dere, K. P., Rich, N. B., & Howard, R. A. 1999, J. Geophys. Res., 104, 22321
Wang, Y.-M., & Sheeley, N. R., Jr. 1992, ApJ, 392, 310
Wang, Y.-M., & Sheeley, N. R., Jr. 2003, ApJ, 599, 1404
Wang, Y.-M., Sheeley, N. R., Jr, & Rich, N. B. 2007, ApJ, 658, 1340
Winterhalter, D., Smith, E. J., Burton, M. E., Murphy, N., & McComas, D. J. 1994, J. Geophys. Res., 99, 6667
Wu, S. T., Guo, W. P., Michels, D. J., & Burlaga, L. F. 1999, J. Geophys. Res., 104, 14789
Zhao, X., & Hoeksema, J. T. 1996, J. Geophys. Res., 101, 4825